Available online at www.sciencedirect.com
SCIENCE DIRECT®
Pergamon
Cement and Concrete Research 34 (2004) 1669–1673
CEMENT AND CONCRETE RESEARCH

Ettringite formation and microstructure of rapid hardening cement

Etsuo Sakai[a,*], Yasuyuki Nikaido[b], Takumi Itoh[a], Masaki Daimon[a]

[a]Department of Metallurgy and Ceramics Science, Tokyo Institute of Technology, 2-12-1 Ookayama, Meguro, Tokyo 152-8552, Japan
[b]Denki Kagaku Kogyo K.K., 1-1-2, Yuraku-cho, Chiyoda, Tokyo 100-8445, Japan

Received 1 October 2003; accepted 12 April 2004

Abstract

This paper reports the formation and microstructure development of ettringite during hydration of two rapid hardening cements under various handling times. The rapid hardening component of one of these cements is crystalline calcium fluoroaluminate while that of the other is an amorphous calcium aluminate. During hydration, the crystalline fluoroaluminate component forms ettringite from the very beginning. The amount of ettringite increases with time producing needle-shaped crystal of various sizes. The amorphous calcium aluminate component, on the other hand, exhibits an initial induction period after which there is a rapid formation of needle-shaped ettringite crystals of nearly uniform size.

Keywords: Ettringite; Hydration; Microstructure; Calcium aluminate cement; Amorphous materials

1. Introduction

In Japan, rapid hardening cements are being used increasingly in a variety of highway repairs. These cements usually have a short handling time of about 20 min, and the compressive strength over 24 MPa can be obtained in about 3 h after mixing. Since 1995, with changes in the freight truck tonnage, there has been much activity on increasing the thickness of highway bridge slab. This work involves large construction equipment placing a rather large volume of rapid hardening cement. The handling time of these cements has to be extended to at least about an hour to perform this type of highway work [1]. The control or manipulation of the handling time of rapid hardening cements has also become necessary with the new developments in tunneling and repair and reinforcing methods [2]. It is, therefore, important and useful, from the material design viewpoint [3], to understand and clarify the effect of extending handling time on the hydration and microstructure development of these rapid hardening cements.

Two types of rapid hardening cements are used in this study. The rapid hardening component of one of them is a crystalline calcium fluoroaluminaete while that of the other is an amorphous calcium aluminate. Both react with anhydrite during hydration to produce ettringite. The hydration of rapid hardening cements has been investigated in detail by Uchikawa and Uchida [4] and Nakagawa [5]. However, little information is available on the quantitative comparison of the abovementioned rapid hardening cements, particularly, regarding their hydration behavior and microstructure development under extended handling times. This study is aimed to provide information on the formation and microstructure development of ettringite in the initial stages of hydration and hardening of these two types of cements under various handling times.

2. Experimental

2.1. Materials

Table 1 shows the chemical composition and physical characteristics of the two rapid hardening cements investigated. The main rapid hardening component of Type A is crystalline calcium fluoroaluminaete while that of Type B is an amorphous calcium aluminate. A set retarder consisting of hydrocaboxylic acid and sodium carbonate was used with both cements.

* Corresponding author. Tel.: +81-3-5734-3368; fax: +81-3-5734-2862.
E-mail address: esakai@ceram.titech.ac.jp (E. Sakai).

0008-8846/$ – see front matter © 2004 Elsevier Ltd. All rights reserved.
doi:10.1016/j.cemconres.2004.04.021

Table 1
Chemical and physical properties of rapid hardening cements

Cement	Chemical composition (%)									Rapid hardening component	Specific gravity	SSA[a] (cm^2/g)
	Ignition loss	SiO_2	Al_2O_3	Fe_2O_3	CaO	MgO	SO_3	R_2O	F			
Type A	0.6	13.8	11.4	1.5	59.1	0.9	10.2	0.7	1.2	$C_{11}A_7{\cdot}CaF_2$	3.03	5500
Type B	2.1	15.6	9.5	2.1	58.5	0.6	9.7	0.9	0	Amor-$C_{12}A_7$	3.03	4670

[a] Blane's specific surface area.

2.2. Sample preparation

To stop the hydration of the cements investigated, it was important to select a method that would not result in the decomposition of ettringite. We tested several methods using synthetic ettringite [6]. Treating cement paste with acetone followed by drying for 16 h at 40 °C was found to be the most suitable method.

2.3. Cement hydration

To prolong the handling time of hardening cements, the retarder was added, by mass of cement, in amounts of 0.2%, 0.7% and 1.2% to Type A cement, and 0.7% and 1.0% to Type B cement. This dosage resulted in the handling times of 30, 60 and 120 min (referred to as HT30, HT60 and HT120, respectively, in Figs. 1–5) for both cements. The retarder was added by dissolving it in the mixing water. A water-to-cement ratio of 0.5 was used in all experiments. Conduction calorimeter was used to obtain heat liberation curves during hydration.

The cement samples were hydrated and cured in the bottles made of polystyrene at 22 °C. The hydration was stopped after a prescribed time (5, 30, 60, 90, 120, 180 and 300 min) by mixing the sample with a large quantity of acetone and milling in an alumina mortar. The sample was then filtered under reduced pressure and dried for 16 h in a thermostat at 40 °C.

2.4. Quantitative analysis

The amount of ettringite produced during hydration was determined by quantitative X-ray diffraction (XRD) using 10 mass % α-alumina as the internal standard. The ettringite peak area was determined using the method of numerically integrating functions fitting the peak profile obtained by XRD. The amount of ettringite produced was determined by comparing its peak area with that of pure synthetic ettringite (taken 100%). The ignition loss was determined by heating the samples at 1000 °C for 30 min.

2.5. Microstructure

The microstructure of hydrated samples was examined by scanning electron microscopy (SEM), and their pore size distribution was determined by mercury (Hg) porosimetry.

3. Results and discussion

3.1. Rate of heat liberation

Figs. 1 and 2 show the heat liberation curves for Type A and B cements, respectively. For Type A, the hydration appears to begin immediately upon mixing the cement with water, as shown by a rapid heat liberation, which is then followed by two more reaction stages (Fig. 1). Ettringite

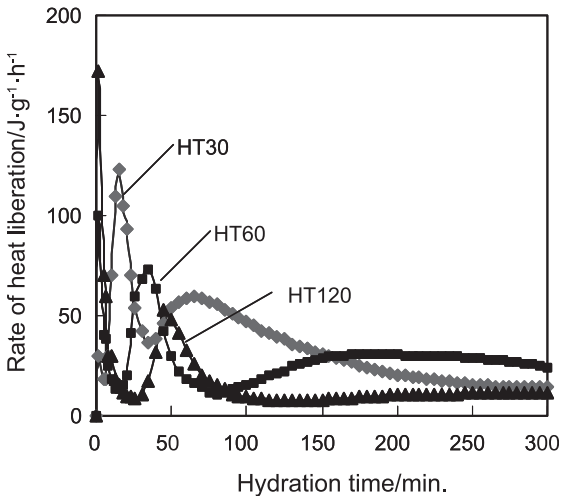

Fig. 1. Heat liberation curves for Type A cement.

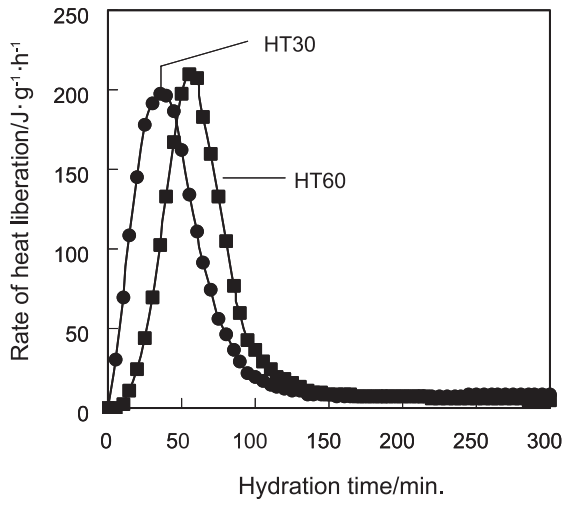

Fig. 2. Heat liberation curves for Type B cement.

was the only product detected by XRD. Increasing the retarder dosage delayed the second and third peaks in the heat liberation curve. For Type B cement, on the other hand, there was no heat generation immediately after addition of water, and only a large exothermic peak was noticed (Fig. 2). Ettringite was detected by XRD at around the time of the middle of this exothermic peak. This peak is produced presumably by the dissolution of amorphous calcium aluminate and anhydrite and the formation of ettringite. With increased retarder dosage, the time of appearance of this peak is delayed (i.e., a prolonged induction period is observed), but its size remains relatively unaffected. Amorphous calcium aluminate, the rapid hardening component of Type B cement, shows remarkably high reactivity compared with crystalline calcium aluminate [7]. The restrained reaction in the early hydration of Type B cement, therefore, may be due to some special surface condition introduced by grinding of the amorphous calcium aluminate.

3.2. Ettringite production and microstructure

The amount of ettringite produced during hydration was calculated using the following equation:

$$\text{Ettringite}\ (\%) = 100R_hE_s(100 - L_s)/R_sE_h(100 - L_h)$$

where R_h and R_s are the XRD peak areas of ettringite and internal standard, respectively, for the hydrated sample, and E_h and E_s are the peak areas of ettringite and the internal standard for the synthetic ettringite, respectively. L_h and L_s are ignition losses for the hydrated sample after t min and synthetic ettringite, respectively.

The XRD analysis shows ettringite as the sole hydration product even up to 300 min. The amount of ettringite as determined by XRD is found to be almost the same as that calculated from the ignition loss data (Fig. 3). The ignition loss, therefore, appears to be entirely due to the loss of

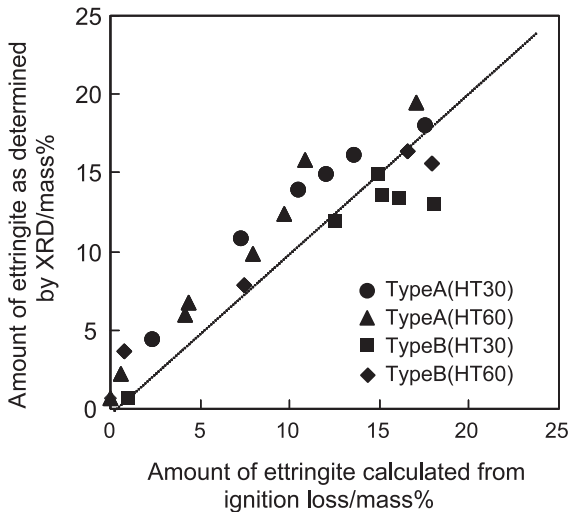

Fig. 3. Relation between the amount of ettringite as determined by XRD and that calculated from the ignition loss data.

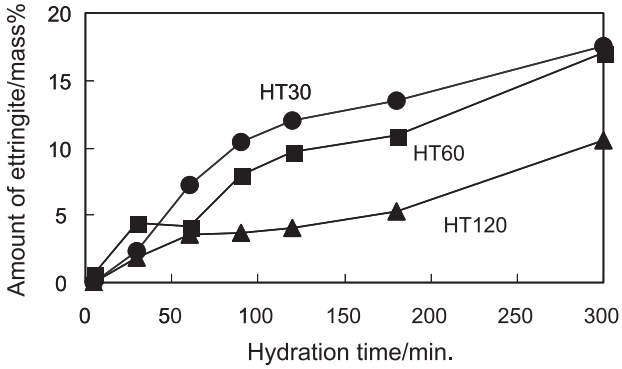

Fig. 4. The amount of ettringite produced by hydration of Type A cement.

combined water in ettringite upon heating. This result also confirms that crystalline materials with orientations, such as needle-shaped ettringite, can be determined quantitatively by XRD, provided care is taken in preparing the samples for measurements.

Figs. 4 and 5 show the amount of ettringite produced by hydration of Type A and B cements, respectively. In Type A, ettringite is formed from very early stage, and its amount increases gradually with time. Extending the handling time decreases the ettringite formation rate requiring a longer time to produce a certain amount of ettringite. In Type B cement, there appears to be an induction period which is followed by rapid formation of ettringite. Extending the handling time increases the induction period, but does not appear to affect the shapes of the heat liberation curves.

Fig. 6 shows SEM photographs of some of the hydrated cement pastes after 180 min. The handling time for these set samples was 30 min. For Type A, minute needle-shaped ettringite crystals are observed at the beginning of hydration. After 180 min, needle-shaped crystals of various sizes are noticed. For Type B, although no ettringite is detected in the early stages of hydration, a large amount of needle-shaped ettringite crystals of nearly uniform size is observed after 180 min. These micrographs appear to correlate well with Figs. 4 and 5 data regarding ettringite formation with hydration time. In Type A, fine ettringite crystals are formed

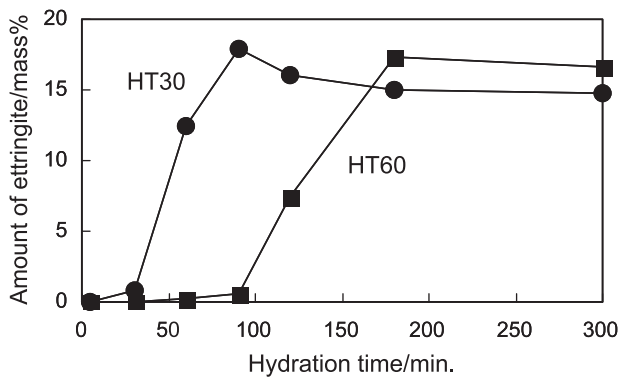

Fig. 5. The amount of ettringite produced by hydration of Type B cement.

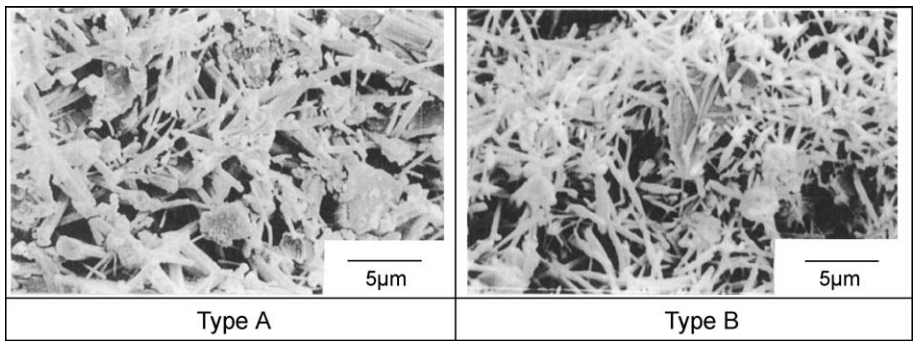

Fig. 6. SEM photographs of hydrated samples (HT30, after 180 min).

immediately after the addition of water, which gradually grow larger in size. In Type B, on the other hand, no ettringite is formed until a certain period of time after the addition of water. However, once ettringite begins to form, it forms rapidly producing crystals of comparatively uniform size.

3.3. Total pore volume of hydrated cement pastes

Figs. 7 and 8 show, respectively, the correlations of total pore volume and threshold diameter for cumulative pore volume of cement pastes with the hydration time. In the case of Type A cement, the threshold diameter shifts to smaller values and the total pore volume decreases with increasing hydration time. The Type B cement shows smaller total pore volume than that the Type A cement at 60 min and its threshold diameter also shifts to smaller values. This threshold diameter does not show any significant variation afterwards.

The changes in total pore volume and threshold diameter in hardened cements can be correlated with ettringite formation during hydration. In Type A cement, the amount of ettringite continues to increase and crystals of various sizes are formed with hydration time with the result that large pores are filled with them. Consequently, both the total pore volume and the threshold diameter decrease with time. In Type B cement, ettringite crystals of comparatively uniform size are formed rapidly in the first stage after which there is very little change. Consequently, at 60 min, both the total pore volume and threshold diameter have smaller values compared with those for Type A. At 180 min, when both cements are expected to show about the same strength, we observed about the same total pore volume. In this instance, the amounts of ettringite produced by Types A and B are 13.4% and 15.2%, respectively, with the result that both cements show very similar values.

4. Conclusions

The two rapid hardening cements used in highway repair work, produce ettringite in their early stages of hydration. However, there is a distinct difference between these cements regarding the mechanisms of ettringite formation and its microstructure. The heat liberation curve for Type A cement shows three stages of reaction. Ettringite is formed immediately after addition of water and its amount continues to increase with time. Extending the handling time

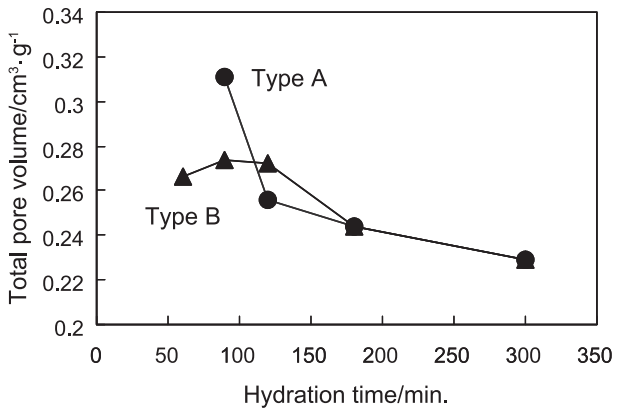

Fig. 7. Total pore volume of hydrated cement pastes.

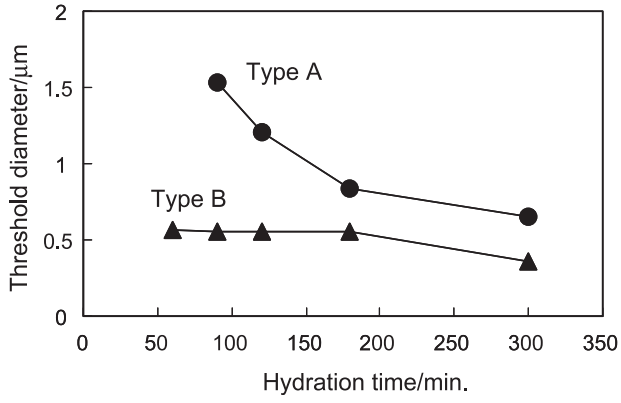

Fig. 8. Threshold diameter for cumulative pore volume of hydrated cement pastes.

decreases the rate of ettringite formation. The heat liberation curve for Type B cement shows only one large exothermic peak. Ettringite begins to form rapidly at around the middle of this peak. There is an induction period in the initial hydration stage which can be prolonged by prolonging the handling time. The Type A cement exhibits ettringite crystal growth of various sizes whereas Type B produces ettringite crystals of nearly uniform size crystals. The total pore volume and threshold diameter of both cements gradually decreases with hydration time; however, these parameters show relatively smaller values for Type B than those for Type A in the initial stages of hydration.

Acknowledgements

The authors would like to thank Dr. Inam Jawed of Trasportation Research Board National Research Council for helpful discussion on the subject.

References

[1] N. Kondo, Y. Nikaido, E. Sakai, M. Daimon, Relation between ettringite formation and the development of strength for rapid hardening cement, Proc. 10th Int'l. Cong. Chemistry of Cement, vol. 2, Amarkai AB and Congrex Göterborg AB, Göterborg, Sweden, 1997, p. 2ii017.
[2] K. Kano, E. Sakai, M. Dimon, Quality control system and prediction of strength from phase composition of very high early strength cement, Cem. Sci. Concr. Tech. 52 (1998) 16–21 (in Japanese).
[3] S. Teramura, Y. Matsunaga, K. Hirano, E. Sakai, Accelerator for shotcrete based amorphous calcium aluminate, Prco. Eng. Found. Conf. Shotcrete for Underground Support, vol. IV, Amer. Soc. Civil Eng., New York, 1993, pp. 9–16.
[4] H. Uchikawa, S. Uchida, The hydration of $11CaO{\cdot}7Al_2O_3{\cdot}CaF_2$ at 20 °C, Cem. Concr. Res. 2 (1972) 681–695.
[5] K. Nakagawa, Working mechanisms of amorphous calcium aluminate and its application for construction materials, PhD Thesis, Tokyo Institute of Technology, 1990, in Japanese.
[6] J.K. Lee, Y. Ohba, E. Sakai, M. Daimon, Synthesis of hydrates for C_3A-$CaSO_4{\cdot}2H_2O$-$CaCO_3$-Na_2SO_4-H_2O system, Inorg. Mater. 4 (1997) 196–204 (in Japanese).
[7] K. Nakagawa, I. Terashima, K. Asaga, M. Daimon, A study of hydration of amorphous calcium aluminate by selective dissolution analysis, Cem. Concr. Res. 20 (1990) 661–665.